

Tracking Reproductivity of COVID-19 Epidemic in China with Varying Coefficient SIR Model

Haoxuan Sun¹, Yumou Qiu², Han Yan³, Yaxuan Huang⁴, Yuru Zhu⁵, Jia Gu⁵ and Song Xi Chen^{6,5}

Abstract

We propose a varying coefficient Susceptible-Infected-Removal (vSIR) model that allows changing infection and removal rates for the latest corona virus (COVID-19) outbreak in China. The vSIR model together with proposed estimation procedures allow one to track the reproductivity of the COVID-19 through time and to assess the effectiveness of the control measures implemented since Jan 23 2020 when the city of Wuhan was lockdown followed by an extremely high level of self-isolation in the population. Our study finds that the reproductibility of COVID-19 has been significantly slowed down in the three weeks from January 27 to February 17th with 96.3% and 95.1% reductions in the effective reproduction numbers R among the 30 provinces and 15 Hubei cities, respectively. Predictions to the ending times and the total numbers of infected are made under three scenarios of the removal rates. The paper provides a timely model and associated estimation and prediction methods which may be applied in other countries to track, assess and predict the epidemic of the COVID-19 or other infectious diseases.

Keywords: Epidemic assessment; Estimation of Basic reproductive number; SIR model; Varying coefficient model;

1: Center for Data Science, Peking University; 2: Department of Statistics, Iowa State University, Joint Corresponding Author; 3: School of Mathematical Sciences, Sichuan University; 4: Yuanpei College, Peking University; 5: Center for Statistical Science, Peking University; 6: Guanghua School of Management, Peking University, Corresponding Author.

1. Introduction

The Corona Virus Disease 2019 (COVID-19) has created a profound public health emergency in China and has spread to 25 countries so far (World Health Organization (WHO), 2020). It has become an epidemic with more than 76,000 confirmed infections and 2,244 reported deaths worldwide as on February 20 2020. The COVID-19 is caused by a new corona viruses that is genetically similar to the viruses causing severe acute respiratory syndrome (SARS) and Middle East respiratory syndrome (MERS). Despite a relatively lower fatality rate comparing to SARS and MERS, the COVID-19 spreads faster and infects much more people than the SARS-03 outbreak.

The city of Wuhan, the origin of the outbreak, has been locked up to reduce population movement since January 23 in an effort to stop the spread of the epidemic, followed by more than 50 prefecture level cities (as on 8th of February) and countless number of towns and villages in China. A high percentage of the population are exercising self-isolation in their homes. The spring festival holiday period had been extended with all schools and universities closed and all students staying where they are indefinitely. The country is virtually in a stand-still, and the economy and people's livelihood have been severely affected by the epidemic.

There is an urgent need to assess the speed of the disease transmission and to check if the existing containment measures have successfully slowed down the spread of the disease or not. The Susceptible-Infected-Removal (SIR) model (Kermack and McKendrick, 1927) and its generalizations, for instance the Susceptible-Exposed-Infected-Removal (SEIR) model (Hethcote, 2000) with four or more compartments are commonly used to model the dynamics of infectious disease outbreaks. See (Becker, 1977; Becker and Britton, 1999; Yip and Chen, 1998; Ball and Clancy, 1993) for statistical estimation and inference for stochastic versions of the SIR model. SEIR models have been used to produce early results on COVID-19 in (Wu et al., 2020; Read et al., 2020; Tang et al., 2020), which produced the first three estimates of the basic reproduction number R_0 : 2.68 by (Wu et al., 2020), 3.81 by (Read et al., 2020) and 6.47 by (Tang et al., 2020). The R_0 is the expected number of infections by one infectious person over his/her infectious period *at the start of the epidemic*, which is closely connected to the effective reproduction number R_t . The latter R_t is the expected number of infections by one infected over infectious period at time t of the epidemic. Both R_0 and R_t are key measures of an epidemic. For fixed coefficient models, if $R_0 < 1$, the epidemic

38 will die down eventually with the speed of the decline depends on the size of
39 R_0 ; otherwise, the epidemic will explode until it runs out of its course.

40 The SEIR models that was employed in the above three cited works for the
41 COVID-19 assume constant model coefficients, implying a constant regime of
42 transmission during the course of the epidemic. This is idealistic for modeling
43 COVID-19 as it cannot reflect the intervention measures by the authorities
44 and the citizens, which should have made the infectious rate (β) and the
45 effective reproduction number (R_t) varying with respect to time. Here, the
46 effective reproductive number R_t is the average number of secondary infec-
47 tions made by each infectious case during an epidemic, which contrasts the
48 basic reproductive number R_0 that measures the average number of secondary
49 infections at the beginning of an epidemic.

50 To reflect the changing dynamic regimes due to the strong government
51 intervention and the self protective reactions by citizens, we propose a varying
52 coefficient SIR (vSIR) model. The vSIR model is easy to be implemented via
53 the locally weighted regression approach (Cleveland and Devlin, 1988) that
54 produces estimates with desired smoothness, and yet is able to capture the
55 changing dynamics of COVID-19's reproduction, with guaranteed statistical
56 consistency and needed standard errors. The consistent estimator and its
57 confidence interval are proposed for estimating the trend of R , assessing the
58 effectiveness of infection control, and predicting the ending time and the final
59 number of infection cases with 95% prediction intervals.

60 As COVID-19 is quickly spreading outside China, the vSIR model and
61 the associated estimation and prediction methods may be applied to other
62 countries to track, assess and predict the epidemic of the COVID-19 or other
63 infectious diseases.

64 **2. Main Results**

65 By applying the vSIR model, we produce daily estimates of the infectious
66 rate $\beta(t)$ and the effective reproduction number R_t^D (t denotes time) based
67 on three values of infectious duration D : 7, 10.5 and 14 days for 30 provinces
68 and 15 major cities (including Wuhan) in Hubei province from January 21
69 or a later date between January 24-29 depending on the first confirmed case
70 to February 17.

- 71 • Despite the total number of confirmed cases and the death are increas-
72 ing, the spread of COVID-19 has shown a great slowing down in China

73 within the two weeks from January 27 to February 17 as shown by
74 96.3% and 95.1% reductions in the effective reproduction number R_t
75 among the 30 provinces and the 15 cities in Hubei, respectively.

76 • The average R_t^{14} (based on 14-day infectious duration) on January 27th
77 was 6.14 (1.49) and 7.59 (2.38), respectively, for the 27 provinces and
78 the 7 Hubei cities with confirmed cases by January 23rd. The numbers
79 in the parentheses are the standard error. One week later on Febru-
80 ary 3rd, the R_t^{14} was averaged at 2.18 (0.67) for the 30 provinces and
81 2.84 (0.59) for the 15 Hubei cities, representing 64.5% and 62.6% re-
82 ductions, respectively, over the 7 days. On February 10th, the average
83 R_t^{14} dropped further to 0.86 (0.38) for the 30 provinces and 1.23 (0.55)
84 for the 15 Hubei cities, which were either below or close to the critical
85 threshold level 1.

86 • On February 17th, the average R_t^{14} has reached 0.23(0.15) and 0.37(0.24)
87 for the 30 provinces and the 15 Hubei cities, with 22 provinces' and 8
88 Hubei cities' R_t^{14} being statistically significantly below 1 for more than
89 7 days. These indicate a further slowing down in the re-productivity
90 of COVID-19 in China in the week from February 10 to 17.

91 • The profound slowing down in the reproductivity of COVID-19 can
92 be attributed to a series of containment measures by the government
93 and the public, which include cutting off Wuhan and other cities from
94 January 23, a rapid public awareness of the epidemic and the extensive
95 self protection taken and high level of self isolation at home exercised
96 over a much extended Spring Festival holiday period.

97 • There are increasing numbers of provinces and cities in Hubei whose
98 14-day R_t has been statistically below 1, as detailed in Table 1, which
99 would foreshadow the coming of the turning point for containment of
100 the epidemic, if the control measures implemented since January 23
101 can be continued.

102 • If the recovery rate can be increased to 0.1 meaning the average recover
103 time is 10 days after diagnosis, the number of infected patients $I(t)$ will
104 be dramatically reduced in March, and the epidemic will end in April
105 for non-Hubei provinces and end in June for Hubei.

106 **3. Time-varying coefficient SIR model**

107 Let $S(t)$, $I(t)$ and $R(t)$ be the counts of susceptible, infected and removed
 108 (including dead) persons in a given city or province at time t , respectively.
 109 Let N be the total population of the city/province. We propose a varying
 110 coefficient Susceptible-Infected-Removed (vSIR) model for the conditional
 111 means of the Poisson increments $\Delta I(t)$ and $\Delta R(t)$ given $I(t)$ and $R(t)$. This
 112 vSIR-Poisson framework permits estimating the parameters and the effective
 113 reproduction number R_t for the dynamics of COVID-19, which are then used
 114 for predicting the future spread of the disease.

115 The SIR model (Kermack and McKendrick, 1927) is a commonly used
 116 epidemiology model for the dynamic of susceptible $S(t)$, infected $I(t)$ and
 117 recovered $R(t)$ as a system of ordinary differential equations (ODEs). Here
 118 we consider a generalized version of the SIR model in that the infectious
 119 rate β and the removal rate γ may vary with respect to time so that the
 120 deterministic ODEs are

$$\begin{aligned} \frac{dS(t)}{dt} &= -\beta(t)I(t)\frac{S(t)}{N}, \\ \frac{dI(t)}{dt} &= \beta(t)I(t)\frac{S(t)}{N} - \gamma(t)I(t), \\ \frac{dR(t)}{dt} &= \gamma(t)I(t), \end{aligned} \tag{1}$$

121 where $\beta(t)$ and $\gamma(t)$ are unknown infection and the removal rate functions,
 122 respectively. Once an individual is removed, including dead, the individual
 123 can not return to the susceptible group.

124 The rationale for using a time-varying $\beta(t)$ function, rather than a con-
 125 stant β , is that $\beta(t)$ is the average rate of contact per unit time multiplied
 126 by the probability of disease transmission per contact between a suscepti-
 127 ble and an infectious subject. Due to an increasing public awareness of the
 128 epidemic and the control measures as mentioned earlier, both the transmis-
 129 sion probability and the contact rate have been largely reduced. These favor
 130 for a time-varying $\beta(t)$, which are also confirmed by the sharp declined in
 131 $R_t^D = \beta(t)D$, where D denote the infectious durations in Figures 1 and 2.
 132 The removal rate also changes over time as treatments improve over time as
 133 shown in Figure 3. However, Figure 3 shows $\gamma(t)$ is much slowly changing
 134 for most of the provinces, which led us to treat $\gamma(t) = \gamma$ at the early stage of
 135 the outbreak, whose value gradually increased as the recover rate improved
 136 as the time progress and better treatments are available.

137 The deterministic vSIR model as specified by the ODEs in (1) speci-
 138 fies the conditional means of the Poisson increments $\Delta I(t)$ and $\Delta R(t)$ given
 139 $S(t)$, $I(t)$ and $R(t)$ at each discrete time point t . This conditional mean
 140 specification leads to a Poisson-vSIR model framework, which can be used
 141 to construct conditional likelihood for $(\beta(t), \gamma(t))$ over moving time windows
 142 and leads to statistical inference for the effective reproduction ratio estima-
 143 tion and its standard error. The Poisson-vSIR framework is also the basis
 144 for the bootstrap re-sampling algorithm that we will propose for generating
 145 predictive intervals.

146 SEIR model is an extension of SIR with an added compartment E for the
 147 exposed between S and I . A time-varying SEIR model (vSEIR) satisfies the
 148 ODEs

$$\begin{aligned}
 \frac{dS(t)}{dt} &= -\beta(t)I(t)s(t), \\
 \frac{dE(t)}{dt} &= \beta(t)I(t)s(t) - \alpha(t)E(t), \\
 \frac{dI(t)}{dt} &= \alpha(t)E(t) - \gamma(t)I(t), \\
 \frac{dR(t)}{dt} &= \gamma(t)I(t),
 \end{aligned}
 \tag{2}$$

149 where $\alpha(t)$ is the confirmation or diagnosis rate from E to I . The ODEs in
 150 (2) specifies the conditional means of the independent Poisson increments.
 151 However, like SIR model, the states before I are not infectious.

152 The basic and the effective reproduction numbers (RN), R_0 and R_t , are
 153 important notions in epidemiology as they quantify the reproduction ability
 154 of an epidemic at the start (R_0) and during (R_t) an epidemic. For both SIR
 155 and SEIR models, $R_0 = R = \beta/\gamma$ (Hethcote, 2000). We are to demonstrate
 156 that for the vSIR model, $R_0 = \beta(0)/\gamma(0)$ and the effective RN $R_t = \tilde{\beta}(t)/\gamma(t)$
 157 at time t where $\tilde{\beta}_t = \beta(t)s(t)$ and $s(t) = S(t)/N$. The susceptible rate $s(t)$
 158 is approximately 1 at the start of an epidemic. However, $s(t) < 1$ has to be
 159 taken into account as the number of susceptibles declines.

160 Figure 4 provides the vSIR and vSEIR epidemic progression networks
 161 from an initial $I(0)$ infected and initial $I(0)$ and $E(0)$ infected, respectively.
 162 The figure also provides the According to the Poisson-vSIR model, at the
 163 start of the epidemic, conditioning on $I(0)$, in average $I(1) = (1 - \gamma(0) +$
 164 $\tilde{\beta}(0))I(0) > I(0)$ if and only if $1 - \gamma(t - 1) + \tilde{\beta}(t - 1) > 1$, which is if and
 165 only if $R_0 = \tilde{\beta}(0)/\gamma(0) > 1$. In general, at time t , conditioning on $I(t - 1)$,

166 in average $I(t) = (1 - \gamma(t - 1) + \tilde{\beta}(t - 1))I(t - 1) > I(t - 1)$ if and only if
167 $1 - \gamma(t - 1) + \tilde{\beta}(t - 1) > 1$, which is the case iff the effective RN $R_{t-1} > 1$.
168 Thus, indeed, R_t can track the trend of an epidemic being expanding or
169 shrinking. A similar argument can be made under the vSEIR model.

170 4. Data

171 Daily records of infected, dead and recovered patients released by National
172 Health Commission of China (NHCC) are obtained from the NHCC website,
173 with the first confirmed record for Wuhan on December 8th, 2019, followed
174 by 30 provinces in mainland China and 15 cities in Hubei province where
175 Wuhan is the capital city. We did not consider data from Tibet due to very
176 small number of cases. Due to severe under-reporting in the first 39 days
177 of the epidemics in Wuhan and Hubei, we consider data from January 16th
178 for Wuhan and Hubei. For other provinces and Hubei cities, the starting
179 dates for data are those of first confirmed case, and the analysis date starts
180 four days after to accommodate the estimation approach for the infectious
181 rate $\beta(t)$. The latest start data for analysis was January 29th for Qinghai
182 province and three cities in Hubei province. The second last analysis starting
183 date was January 28th with two provinces and five Hubei cities. Table A1 in
184 the Supplementary Information (SI) provides the starting dates of the data
185 records and analysis for each province and Hubei city.

186 To guide for the choice of the infectious duration D used when calculating
187 the reproduction number, we consider two public data sources. The first one
188 is obtained in *Shenzhen Government Online*, which contain datasets released
189 by the Shenzhen Municipal Health Commission from January 19th to Febru-
190 ary 13th (Shenzhen Municipal Affairs Service Data Administration, 2020).
191 One dataset provides information on the confirmed cases that include the
192 time of onset, time of hospital admission, cause of illness and other informa-
193 tion of 391 cases, consisting 188 males and 203 females. The admission time
194 of these cases ranged from January 9th to February 11th. Another Shen-
195 zhen dataset reports the discharge times for 94 recovered cases, contained in
196 the former dataset. The second data source comes from Shaoyang Municip-
197 al Health Committee (Shaoyang Municipal Health Commission, 2020) with
198 a dataset of 100 confirmed cases released on February 14 that includes 48
199 male and 52 female patients with the onset dates ranging from January 12
200 to February 11.

201 **5. Estimation and Confidence Intervals**

202 The reported numbers of infected $I(t)$ and removed cases $R(t)$ are subject
 203 to measurement errors. To reduce the errors, we apply a three point moving
 204 average filter on the reported counts to obtain $\bar{I}(t) = 0.3I(t-1) + 0.4I(t) +$
 205 $0.3I(t+1)$ for $2 \leq t \leq T-1$ where T is the latest time point of observation.
 206 In our analysis, T was February 20 of 2020,. For $t = 1$ or T , we apply two
 207 point averaging with $7/10$ weight at $t = 1$ or T , and $3/10$ for $t = 2$ or $T-1$.
 208 Apply the same filtering on the recovered process $R(t)$ and obtain $\bar{R}(t)$. To
 209 simplify the notation, we denote the filtered data $\bar{I}(t)$ and $\bar{R}(t)$ as $I(t)$ and
 210 $R(t)$ respectively, wherever there is no confusion.

211 Hubei started to report the “clinically diagnosed” cases on February 12th
 212 (13th for city Xianning) which created spikes in the newly reported cases.
 213 We applied a one-off linear filter that re-distributes the spikes in the Hubei
 214 cities and Hubei to the previous 7 days with decreasing weights ranging from
 215 $7/28$ to $1/28$.

216 Let $N(t) = I(t) + R(t)$ denotes the cumulative number of diagnosed cases
 217 and $\Delta N(t) = N(t+1) - N(t)$ denotes the daily change. Let $I(t+1, t+1)$
 218 be the newly infected case at date $t+1$. Then, $\Delta R(t) = R(t+1) - R(t) =$
 219 $I(t) - I(t+1) + I(t+1, t+1)$ and $\Delta N(t) = \Delta I(t) + \Delta R(t) = I(t+1, t+1)$
 220 which is the newly infected cases. Thus, conditional on $I(t)$, $(\Delta N(t), \Delta R(t))$
 221 are conditionally independent Poisson random variables. There is a slight
 222 confusion between $N(t)$ and N , as the latter is used to denote the total
 223 population size.

224 We consider the likelihood for the vSIR-Poisson process framework for
 225 parameter estimation by treating β and γ as fixed and later we will relax it
 226 to allow they vary over a window of time t . Then,

$$\Delta N(t) \sim \text{Poisson} \{ \beta(t)S(t)I(t)/N \} \text{ and } \Delta R(t) \sim \text{Poisson} \{ \gamma I(t) \}.$$

227 The likelihood function for $(\Delta I(t), \Delta R(t))$ given $I(t)$ and $R(t)$ is

$$L(\beta, \gamma) = f_1(\Delta N(t)|I(t)) \times f_2(\Delta R(t)|I(t)) \tag{3}$$

228 where f_1 and f_2 are the conditional Poisson density functions. The log like-
 229 lihood based on the increments at t is

$$l(\beta, \alpha, \gamma) \propto -\beta(t)s(t)I(t) + \Delta N(t) \log\{\beta(t)s(t)I(t)\} - \gamma(t)I(t) \\ + \Delta R(t) \log\{\gamma(t)I(t)\}.$$

230 As the population of each province/city is large and the number of total
 231 infected patients is still relatively small, the ratio $S(t)/N$ appeared in (1) is
 232 very close to 1. By approximating $S(t)/N = 1$, the likelihood score equations
 233 are

$$\frac{\partial l}{\partial \beta} = -I(t) + \frac{\Delta N(t)}{\beta(t)s(t)} \quad (4)$$

$$\frac{\partial l}{\partial \gamma} = -I(t) + \frac{\Delta R(t)}{\gamma(t)} \quad (5)$$

234 It can be checked that the score functions have (approximate) zero means.
 235 The approximation of $S(t)/N = 1$ is just to simplify the expression as every-
 236 thing carries through by using $\tilde{\beta}(t) = \beta(t)s(t)$.

237 While one can use the above likelihood based inference, an equivalent
 238 approach we use in our analysis is based on the (approximate) solution for
 239 $I(t)$ via (6)

$$I(t) \approx I(t_1) \exp\{(\beta(t) - \gamma)(t - t_1)\}, \quad (6)$$

240 for $t_1 = t - w + 1, \dots, t$ and a window $w > 0$ which satisfies $w \rightarrow 0$ and $Tw \rightarrow$
 241 ∞ . Here T is the total number of observational time for the processes. Take
 242 logarithm transform on (6), $\log\{I(t)\} \approx \log\{I(t_1)\} + (\beta(t) - \gamma)(t - t_1)$. We
 243 propose estimating $\beta(t) - \gamma$ by a local linear regression of $\log\{I(t)\}$ on $t - t_1$.
 244 The above log-linear regression may be viewed as a version of the Poisson
 245 increment mean model by noting that $\log\{I(t)\} - \log\{I(t_1)\} \approx \frac{I(t) - I(t_1)}{I(t_1)}$ which
 246 is approximately $(\beta(t) - \gamma)(t - t_1)$ in the mean.

247 Let $\widehat{\beta(t) - \gamma}$ be the estimated slope from the local linear regression, and
 248 $\widehat{\text{Var}}(\beta(t) - \gamma)$ be the estimated variance of $\widehat{\beta(t) - \gamma}$. Their close form expres-
 249 sions are provided in Section S.1 in SI.

250 Let $\Delta_\delta R_t = R_{t+\delta} - R_t$ for $t = 1, \dots, T - \delta$. From the second score equation
 251 (5), we estimate $\gamma(t)$ by the local least square fitting of $\Delta_\delta R_t$ on $I(t)$ without
 252 intercept. Let $\hat{\gamma}(t)$ and $\widehat{\text{Var}}(\hat{\gamma})$ be the estimator of γ and its corresponding
 253 estimated variance, respectively. Their expressions are provided in SI. Then,
 254 $\hat{\beta}(t) = \widehat{\beta(t) - \gamma} + \hat{\gamma}$ is the estimate for the varying coefficient $\beta(t)$ in (1).
 255 The standard error of $\hat{\beta}(t)$ can be obtained as $\text{SE}_\beta(t) = \{\widehat{\text{Var}}(\beta(t) - \gamma) +$
 256 $\widehat{\text{Var}}(\hat{\gamma}) + 2\text{Cov}(\widehat{\beta(t) - \gamma}, \hat{\gamma})\}^{1/2}$. The 95% confidence interval for $\beta(t)$ can be
 257 constructed as

$$(\hat{\beta}(t) - 1.96\text{SE}_\beta(t), \hat{\beta}(t) + 1.96\text{SE}_\beta(t)). \quad (7)$$

258 In the implementation, we chose $\delta = 1$ and $w = 5$.

259 To assess the goodness of fitting, Figure S1 in SI shows the observed
260 infected number $I(t)$ versus the fitted values by the proposed varying coef-
261 ficient SIR model for 30 provinces in China. It demonstrates the proposed
262 method is well suitable for the dynamics of COVID-19 outbreak. Figure S2
263 in SI plots the estimated the effective reproductive number R_t^{14} , calculated as
264 $R_t^{14} = \hat{\beta}(t) \times 14$, with its 95% confidence interval for 30 provinces in China.

265 6. Effective Reproduction Number

266 The effective reproduction number R_t is the most important parameter
267 in determining the state of an epidemic. It measures the average number
268 of infection made by an infectious person during the course of his/her being
269 infectious. If $R_t < 1 (> 1)$ for t larger than a t_0 , then the epidemic will
270 die down eventually (explode). There are two widely adopted definitions of
271 $R(t)$. One is based on the average duration of infection of the disease, and
272 the other is via the removal rate $\gamma(t)$.

273 At a date t , the effective reproduction number based on an average infec-
274 tious duration D is $R_t^D = \beta(t)D$ where $\beta(t)$ is the daily infection rate at t .
275 We do not adopt the version involving γ , the removal rate, since its estima-
276 tion is highly volatile at the early stage of an epidemic. A general version of
277 $R(t)$ may be defined as $\int_{t-D_1}^{t+D_2} \beta(u)du$ where positive D_1 and D_2 represent the
278 infectious durations before and after diagnosis, respectively. The R_t^D given
279 above can be viewed as an approximation by the Mean Value Theorem in
280 calculus with $D = D_1 + D_2$.

281 Research works (Li et al., 2020; Guan et al., 2020; Chen et al., 2020) so far
282 on COVID-19 have informed a range of duration for incubation, from onset
283 of illness to diagnosis and then to hospitalization. The average incubation
284 period from the three studies ranged from 3.0 to 5.2 days; the median dura-
285 tion from onset to diagnosis was 4 days (Guan et al., 2020); and the mean
286 duration from onset to first medical visit and then to hospitalization were
287 4.6 and 9.1 days (Li et al., 2020), respectively. Based on a data sample of
288 391 cases from Shenzhen, the average incubation period was 4.46 (0.26) days
289 and the average duration from onset to hospitalization were 3.9 (0.19) days,
290 respectively, where standard error is reported in the parentheses. Another
291 dataset of 100 confirmed cases in Shaoyang (Hunan Province) revealed the
292 average durations from onset to diagnosis and from diagnosis to discharge

293 were 5.67 (0.39) and 10.12 (0.43) days, respectively. There is a recent revela-
294 tion (Guan et al., 2020) that asymptomatic patients can be infectious, which
295 would certainly prolong the infectious duration.

296 There are much variation in the medical capability in timely diagnosis and
297 hospitalization (thus quarantine) of the infected across the country. Thus,
298 the infectious duration D would vary among the provinces and cities, and
299 would change with respect to the stage of the epidemic as well.

300 Given the diverse range of infectious duration across the provinces and
301 cities, in order to standardize and make the effective reproduction number R_t
302 readily comparable, we calculated the R_t^D based on three levels of D : 7, 10.5
303 and 14 days, which represent three scenarios of responsiveness in diagnosing,
304 hospitalization and hence quarantine of the infected. Calculation of the R_t
305 at other duration can be made by inflating or deflating a R_t^D proportionally
306 to reflect a local reality.

307 7. Reproductivity of COVID-19 in China

308 By calculating the time-varying infection rate function $\beta(t)$, we present
309 in Figures 1 the time series of estimated R_t^D at the three levels of D for
310 the 30+15 provinces/cities from late January to February 17th. Figure 2
311 displays four cross sectional R_t^{14} and their confidence intervals on January
312 27th, February 3rd, 10th and 17th, respectively.

313 Figure 1 reveals a monotone decreasing trend for almost all the provinces
314 and cities with only exceptions for Hubei, Guizhou, Jinlin, Neimenggu and
315 Qinghai. Even for those exceptional provinces, the recent trend is largely de-
316 clining. The non-monotone pattern for non-Hubei provinces were largely due
317 to relative small number of infected cases and waves of introduced infections.
318 However, the one for Hubei and Wuhan suggests low data quality and in par-
319 ticularly under reporting and reporting delay. The epidemic statistics from
320 Hubei and the city of Wuhan before January 21th were severely incomplete
321 and with irregular patterns, as millions of people fled from Wuhan before the
322 lockdown. This was the reason we start Hubei's analysis from January 21th.

323 The average R_t^{14} among the 27 provinces (with confirmed cases on and
324 prior to January 23rd) was 6.14 (1.49), and 7.59 (2.38) for 7 of the 15 Hubei
325 cities on January 27. These levels were comparable to the level of R (6.47)
326 given in (Tang et al., 2020).

327 One week later on February 3rd, R_t^{14} was averaged at 2.18 (0.67) for the
328 30 provinces and 2.84 (0.59) for the 15 Hubei cities, indicating that cutting

329 off Wuhan and other cities, and the start of wearing face masks and self
330 isolation at home from January 23th had contributed to 64.5% and 62.6%
331 reduction in the R_t^{14} . In the following week starting from February 4th, the
332 average R_t^{14} came down to 0.86 (0.38) for the 30 provinces and 1.23 (0.55) for
333 the 15 Hubei cities on February 10th, representing further 60.5% and 56.7%
334 reductions, respectively, during the second week. This reflects the beneficial
335 effects of the continued large scale self-isolation within the extended spring
336 festival holiday period.

337 Table 1 provides the reproduction number R_t^D at the two durations on
338 February 10th. It shows that 5 provinces and 5 Hubei cities' R_t^{14} were signifi-
339 cantly above 1 (at 5% significance level). There are 14 provinces and 2 Hubei
340 cities' R_t^{14} were significantly below 1, which were 1 and 1 more than those a
341 day earlier on February 9th, and 9 and 2 more than those on February 8th,
342 respectively. If we use the shorter $D = 10.5$, 22 provinces and 11 Hubei cities
343 had been significantly below 1 for 1-7 consecutive days. These indicated that
344 the reproduction number R_t has showed signs of crossing below the critical
345 threshold 1 in increasing number of provinces and cities in Hubei around
346 February 8-10. An updated Table 1 for February 17th are available in Table
347 2, which showed further improvement since February 10.

348 On February 17th, R_t^{14} of all provinces and cities under consideration
349 have all been statistically significantly below 1, among which 22 provinces
350 and 8 Hubei cities had been for at least seven consecutive days.

351 Given the significant decline in the reproduction numbers, it was time to
352 discuss the turning point for COVID-19 for China. If a province or city's R_t^D
353 started to be below 1 significantly (at 5% level), we would say the province
354 or city have showed signs of the turning point. Given the uncertainty with
355 the data records, especially those large variation in daily infected numbers
356 coming out of Wuhan and Hubei, the turning point of the epidemic would
357 be confirmed if R_t^D have been significantly below 1 for D_1 days, where D_1
358 is the period of infection before diagnosis, assuming all diagnosed cases can
359 be quarantine immediately. Based on the results in (Li et al., 2020; Guan
360 et al., 2020; Chen et al., 2020), $D_1 = 7$ may be considered. Then, based on
361 this criterion, some of the 30+15 provinces/cities had already reached the
362 turning point on February 17, and more would follow in the coming days
363 according to latest Table 2

364 **8. Prediction for Infection Rate and State Variables**

365 As $R_t^D = \beta(t)D$, predicting $\beta(t)$ is equivalent to predicting R_t^D . From
 366 Figure 1 and Figure S2 in SI, we see that the overall trends of $\beta(t)$ is de-
 367 creasing. But the rate of decreasing gets smaller as time travels. To model
 368 such trend, we consider the reciprocal regression

$$\beta(t) \hat{=} \frac{b}{t^\eta - a} + e_t \quad (8)$$

369 with error e_t and unknown parameters a , b and η . The parameters a and b are
 370 estimated by minimizing the sum-of-squares distance between the estimates
 371 $\hat{\beta}(t)$ and their fitted values for a given η , and then the optimal η is chosen to
 372 be the one that gives the minimum mean square error over a set of candidate
 373 values from 0.5 to 5 with 0.1 increment. Let \tilde{a} , \tilde{b} and $\tilde{\eta}$ be the estimated
 374 parameters, and $\tilde{\beta}(t) = \tilde{b}/(t^{\tilde{\eta}} - \tilde{a})$ be the fitted function. Figure S3 in SI
 375 shows the reciprocal model fits $\hat{\beta}(t)$ quite well for most of the provinces,
 376 especially those with large number of infected cases.

377 With the fitted $\tilde{\beta}(t)$, we project $\{S(t), I(t), R(t)\}$ via the ODEs

$$\begin{aligned} \frac{d\hat{S}(t)}{dt} &= -\tilde{\beta}(t)\hat{I}(t)\frac{\hat{S}(t)}{N}, \\ \frac{d\hat{I}(t)}{dt} &= \tilde{\beta}(t)\hat{I}(t)\frac{\hat{S}(t)}{N} - \hat{\gamma}_T\hat{I}(t), \\ \frac{d\hat{R}(t)}{dt} &= \hat{\gamma}_T\hat{I}(t). \end{aligned} \quad (9)$$

378 where $\hat{\gamma}_T$ is the estimated recovery rate at time T using the last five days'
 379 data. With the observed $\{S(T), I(T), R(T)\}$ at the current time T as the
 380 initial values, numerical solutions $\{(\hat{S}(t), \hat{I}(t), \hat{R}(t)) : T \leq t < \infty\}$ for the
 381 system (9) could be obtained using the Euler method. Then, the end time of
 382 the epidemic can be predicted as $t_{\text{end}} = \min\{t : \hat{I}(t) < 1\}$, and the estimated
 383 final infected number is $\hat{N}_{\text{final}} = \hat{R}(t_{\text{end}}) + \hat{I}(t_{\text{end}})$.

384 To conduct statistical inference for the epidemic predictions, we use the
 385 bootstrap method. In particular, we generate parametric bootstrap resam-
 386 pled processes based on the vSIR model which facilitate the construction of
 387 prediction intervals. We regard that the increments of $S(t)$ and $R(t)$ follow
 388 the Poisson processes (Bretó et al., 2009) over time as

$$-\Delta S(t) \sim \text{Poisson}\{\beta(t)S(t)I(t)/N\} \text{ and } \Delta R(t) \sim \text{Poisson}\{\gamma I(t)\}$$

389 where $\Delta S(t) = S(t+1) - S(t)$ and $\Delta R(t) = R(t+1) - R(t)$. With the esti-
 390 mated $\hat{\gamma}$ and $\hat{\beta}(t)$, we generate bootstrap samples $\{(S^{(b)}(t), I^{(b)}(t), R^{(b)}(t))\}_{t=1}^T$
 391 of the original process for $b = 1, 2, \dots, B$.

For each bootstrap resampled $\{(S^{(b)}(t), I^{(b)}(t), R^{(b)}(t))\}_{t=1}^T$, we obtain the
 estimates $\beta_{\star}^b(t)$ and γ_{\star}^b for $\beta(t)$ and γ in the same way as for the original
 sample. Let $\bar{\beta}_{\star}(t) = \sum_{b=1}^B \beta_{\star}^b(t)/B$ and $\bar{\gamma}_{\star} = \sum_{b=1}^B \gamma_{\star}^b/B$ be the average of
 the bootstrap estimates. We employ the bias corrected bootstrap estimates
 for $\beta(t)$ and γ as

$$\hat{\beta}^b(t) = \hat{\beta}(t) + (\beta_{\star}^b(t) - \bar{\beta}_{\star}(t)) \quad \text{and} \quad \hat{\gamma}^b = \hat{\gamma} + (\gamma_{\star}^b - \bar{\gamma}_{\star})$$

392 for $b = 1, 2, \dots, B$. We then use the reciprocal model (8) to project the
 393 future path of $\hat{\beta}^b(t)$, and use the numerical solution of the vSIR ODEs to
 394 predict the end time and the accumulative number of final infected cases as
 395 we described in section 3.4. Let the bootstrap estimates for the peak time be
 396 $\{t_{\text{end}}^b\}_{b=1}^B$. The 95% prediction interval for the peak time is constructed as the
 397 2.5% and 97.5% quantiles of $\{t_{\text{end}}^b\}_{b=1}^B$. Similar bootstrap prediction intervals
 398 can be constructed for the final accumulative infection number N_{final} of the
 399 epidemic.

400 9. Prediction Results

401 Based on the estimated $\beta(t)$ over time, we predict COVID-19's future
 402 trajectories as solutions to the vSIR model. We used data up to February 19
 403 2020 for the prediction under three scenarios for the recovery rate γ . One uses
 404 the empirical estimate based on data to February 19th. As an effective cure
 405 for the virus has not been found, the estimated recovery rates are quite low.
 406 Among the provinces with more than 100 infections on February 19, Jiangsu
 407 had the highest recovery rate 0.08, followed by Jiangxi, Hebei, Shanghai,
 408 Shanxi, Chongqing, Henan (0.07). Hubei, the province at the center of the
 409 epidemic, is 0.025. The other scenarios was to choose $\gamma = 1/14$ and $\gamma =$
 410 0.1, which mean the average removal time from diagnosis was 14 and 10
 411 days, respectively, representing improvement in the treatment for COVID-19
 412 patients as time progressed.

413 Tables 3 presents the 95% prediction intervals for the end times of the epi-
 414 demic and the cumulative number of infected at the ending. The trajectories
 415 of $I(t)$ of the proposed vSIR model are presented in Figure 5 under the three
 416 scenarios of the recovery rate. The predicted infection number $\hat{I}(t)$ is within

417 10% deviation from its observed value based on data up to Feb 19th, see
418 Table A2 in SI for the detailed prediction error. From the trajectory of the
419 vSIR model in Figure 5, for the non-Hubei provinces, the number of infected
420 would quickly decrease in late February and March with very few cases left in
421 April under all the three scenarios. Some provinces with few number of total
422 infected cases may end as early as March (Qinghai, Jilin, Gansu, Ningxia).
423 For Hubei, with a higher recovery rate of 0.1, the duration of the epidemic
424 would be shorten substantially. The ending time for Hubei is around June 20
425 2020 with total number of infection in the range 73,857–74,596. This shows
426 that improving the recovery rate is an efficient way to end the COVID-19
427 infection early given the current decreasing trend of $\beta(t)$, as it leads to the
428 reduction of the infectious duration.

429 10. Discussion

430 The implications of China’s experience in combating COVID-19 to other
431 countries facing the epidemic are two folds. One is to reduce the person-
432 to-person contact rate by self isolation and curtailing population movement;
433 another is to reduce the transmission probability by wearing protective wears
434 when a contact has to be made.

435 The eventual control of COVID-19 is rested on if the existing control mea-
436 sures can be continued further for a period of time. The biggest challenges
437 that can jeopardize the great effort from late January are from the impatient
438 populations eager to get out of the self-isolation driven by either economic
439 needs (migrant workers eager to coming back to cities for income) or people
440 trying to escape from the boredom of self isolation while encouraged by the
441 declining infections in the last two weeks. In any case, the vSIR model and
442 its statistical estimation and inference can be used to model and the assess
443 the COVID-19 epidemics in other countries.

444 References

445 World Health Organization (WHO), Situation report - 26, Avail-
446 able at [https://www.who.int/docs/default-source/coronaviruse/
447 situation-reports/20200215-sitrep-26-covid-19.pdf](https://www.who.int/docs/default-source/coronaviruse/situation-reports/20200215-sitrep-26-covid-19.pdf), 2020. [Ac-
448 cessed February 16, 2020].

449 W. O. Kermack, A. G. McKendrick, A contribution to the mathematical
450 theory of epidemics, Proceedings of the royal society of london. Series A,

- 451 Containing papers of a mathematical and physical character 115 (1927)
452 700–721.
- 453 H. W. Hethcote, The mathematics of infectious diseases, SIAM review 42
454 (2000) 599–653.
- 455 N. G. Becker, On a general stochastic epidemic model, Theoretical Popula-
456 tion Biology 11 (1977) 23–36.
- 457 N. G. Becker, T. Britton, Statistical studies of infectious disease incidence,
458 Journal of the Royal Statistical Society: Series B (Statistical Methodology)
459 61 (1999) 287–307.
- 460 P. S. Yip, Q. Chen, Statistical inference for a multitype epidemic model,
461 Journal of statistical planning and inference 71 (1998) 229–244.
- 462 F. Ball, D. Clancy, The final size and severity of a generalised stochastic
463 multitype epidemic model, Advances in applied probability 25 (1993) 721–
464 736.
- 465 J. T. Wu, K. Leung, G. M. Leung, Nowcasting and forecasting the potential
466 domestic and international spread of the 2019-ncov outbreak originating
467 in wuhan, china: a modelling study, The Lancet (2020).
- 468 J. M. Read, J. R. Bridgen, D. A. Cummings, A. Ho, C. P. Jewell, Novel
469 coronavirus 2019-ncov: early estimation of epidemiological parameters and
470 epidemic predictions, medRxiv (2020).
- 471 B. Tang, X. Wang, Q. Li, N. L. Bragazzi, S. Tang, Y. Xiao, J. Wu, Estimation
472 of the transmission risk of 2019-ncov and its implication for public health
473 interventions, Available at SSRN 3525558 (2020).
- 474 W. S. Cleveland, S. J. Devlin, Locally weighted regression: an approach
475 to regression analysis by local fitting, Journal of the American statistical
476 association 83 (1988) 596–610.
- 477 Shenzhen Municipal Affairs Service Data Administration, Latest data, Avail-
478 able at <https://opendata.sz.gov.cn/data/dataSet/toDataSet>, 2020.
479 [Accessed February 14, 2020].

- 480 Shaoyang Municipal Health Commission, Dynamic information on
481 prevention and control of new coronavirus-infected pneumonia in
482 shaoyang, Available at [https://wjw.shaoyang.gov.cn/wjw/zyxw/
483 202002/c49df53092784c85aaac769149f30265.shtml](https://wjw.shaoyang.gov.cn/wjw/zyxw/202002/c49df53092784c85aaac769149f30265.shtml), 2020. [Accessed
484 February 14, 2020].
- 485 Q. Li, X. Guan, P. Wu, X. Wang, L. Zhou, Y. Tong, R. Ren, K. S. Leung,
486 E. H. Lau, J. Y. Wong, et al., Early transmission dynamics in wuhan,
487 china, of novel coronavirus–infected pneumonia, *New England Journal of
488 Medicine* (2020).
- 489 W. Guan, Z. Ni, Y. Hu, W. Liang, C. Ou, J. He, et al., N. Zhong, Clini-
490 cal characteristics of 2019 novel coronavirus infection in china, *medRxiv*
491 (2020).
- 492 N. Chen, M. Zhou, X. Dong, J. Qu, F. Gong, Y. Han, Y. Qiu, J. Wang,
493 Y. Liu, Y. Wei, et al., Epidemiological and clinical characteristics of 99
494 cases of 2019 novel coronavirus pneumonia in wuhan, china: a descriptive
495 study, *The Lancet* (2020).
- 496 C. Bretó, D. He, E. L. Ionides, A. A. King, et al., Time series analysis via
497 mechanistic models, *The Annals of Applied Statistics* 3 (2009) 319–348.

Table 1: The reproduction number R_t^D at two infectious duration: 10.5 and 14 days, for the 30 mainland provinces and 15 cities in Hubei province on February 10th with extended results on February 17th. The symbols + (−) indicate that the R_t^{14} was significantly above (below) 1 at 5% level of statistical significance, and the numbers inside the square brackets were the consecutive days the R_t^{14} were significantly below 1. The column ΔR gives the percentages of decline in the R_t^{14} from the beginning of analysis to February 10th (the first two weeks of the analysis). The columns $\Delta R(1^{\text{st}})$, $\Delta R(2^{\text{nd}})$ and $\Delta R(3^{\text{rd}})$ are the percentages of decline in the first week (January 27 to February 3rd), the second week (February 3-10), and the third week (February 10-17), respectively.

Province/City	$R_t^{10.5}$	R_t^{14}	ΔR	$\Delta R(1^{\text{st}})$	$\Delta R(2^{\text{nd}})$	$\Delta R(3^{\text{rd}})$
Wuhan	1.99+	2.66+	58.7%	45.9%	23.7%	72.5%
Ezhou	1.64+	2.18+	80%	79.3%	3.6%	67.7%
Hubei	1.48+	1.98+	74.2%	58.2%	38.3%	69.7%
Tianmen	1.33+	1.78+	75%	67.4%	23.4%	52.5%
Guizhou	1.25+	1.67+	62.4%	9.3%	58.5%	91.5%
Xiantao	0.99	1.32	76.9%	46.4%	57%	71.9%
Heilongjiang	0.95	1.27+	81.8%	54.3%	60.3%	62.6%
Hebei	0.94	1.25+	85.4%	82.4%	16.7%	70.5%
Xinjiang	0.9	1.2+	75.6%	60.7%	37.9%	53.1%
Enshizhou	0.86−[5]	1.14+	74.1%	60.3%	34.6%	76%
Jingzhou	0.85−[1]	1.14+	84.8%	50.5%	69.3%	76.9%
Gansu	0.8	1.07	75.1%	47.8%	52.3%	100%
Jingmen	0.79−[1]	1.05	88.3%	77.1%	49.2%	84.1%
Huangshi	0.79−[1]	1.05	78.3%	31.2%	68.4%	83.6%
Anhui	0.74−[1]	0.99	88.3%	71.7%	58.7%	77.6%
Shanxi	0.74−[2]	0.98	86.7%	69.6%	56.1%	87.1%
Ningxia	0.73	0.97	84.9%	75.8%	37.6%	75.7%
Shandong	0.73−[2]	0.97	90.3%	84.5%	37.1%	80.3%
Jiangsu	0.72−[3]	0.96	87.1%	70.5%	56.1%	72.1%
Xianning	0.71−[4]	0.95	70.7%	21.6%	62.6%	33.6%
Shiyan	0.71−[1]	0.94	89.1%	72.4%	60.3%	67.5%
Jilin	0.7	0.93	80.4%	17.6%	76.1%	82.5%
Yichang	0.69−[3]	0.92	87%	56.6%	70%	75.7%
Huanggang	0.69−[3]	0.92	88.9%	60.7%	71.8%	89%
Tianjin	0.69−[4]	0.91	82.9%	51.8%	64.6%	64%
Hainan	0.68−[1]	0.91	80.9%	65.2%	45.2%	96.1%
Guangxi	0.66−[5]	0.88	81.6%	64.9%	47.8%	72.1%
Xiangyang	0.63−[3]	0.84−[1]	88.4%	57.9%	72.4%	80.8%
Sichuan	0.62−[5]	0.83−[2]	89.4%	78.5%	50.7%	47.6%

Continued on next page

Table 1 – continued from previous page

Province/City	$R_t^{10.5}$	R_t^{14}	ΔR	$\Delta R(1^{st})$	$\Delta R(2^{nd})$	$\Delta R(3^{rd})$
Jiangxi	0.61–[2]	0.82	90.8%	70.9%	68.5%	79.6%
Xiaogan	0.6–[1]	0.81	88.9%	61.5%	71.3%	50.1%
Hunan	0.57–[3]	0.76–[2]	91.5%	77%	63.2%	90.4%
Henan	0.56–[2]	0.75–[1]	93.2%	78.8%	67.8%	64.2%
Suizhou	0.52–[2]	0.69–[2]	88.2%	40.9%	80%	65.5%
Chongqing	0.51–[4]	0.68–[3]	90.4%	75%	61.6%	73.9%
Shaanxi	0.51–[3]	0.68–[2]	86.5%	63%	63.6%	72.9%
Neimenggu	0.49–[3]	0.66–[2]	82.4%	43%	69.1%	27.9%
Fujian	0.49–[6]	0.66–[4]	90.5%	76.2%	60%	76.9%
Guangdong	0.45–[3]	0.61–[2]	88.2%	54.4%	74.2%	62%
Liaoning	0.45–[6]	0.6–[2]	89.3%	72.7%	61%	81.7%
Beijing	0.45–[4]	0.6–[2]	90.3%	59.2%	76.2%	65.1%
Shanghai	0.34–[4]	0.46–[2]	92.1%	68%	75.2%	53.4%
Zhejiang	0.31–[4]	0.42–[3]	94.3%	77.9%	74.2%	86.3%
Yunnan	0.28–[7]	0.38–[5]	96.2%	86.8%	71.5%	30.8%
Qinghai	0.02–[4]	0.03–[3]	98.9%	-1.6%	98.9%	100%
Ave(sd)	0.74(0.35)	0.98(0.47)	85.3%	64.2%	59%	71.6%

498

Table 2: The reproduction number R_t^D at two infectious durations: 10.5 and 14, for the 30 mainland provinces and 15 cities in Hubei province on February 17th. The symbols + (–) indicate that the $R_t^{10.5}(R_t^{14})$ was significantly above (below) 1 at 5% level of statistical significance, and the numbers inside the square brackets were the consecutive days the $R_t^{10.5}(R_t^{14})$ were significantly below 1.

Province/City	$R_t^{10.5}$	R_t^{14}
Wuhan	0.55–[9]	0.73–[8]
Ezhou	0.52–[3]	0.69–[2]
Tianmen	0.63–[9]	0.85
Hubei	0.43–[3]	0.56–[2]
Sichuan	0.33–[19]	0.44–[16]
Xiantao	0.28–[14]	0.37–[13]
Tianjin	0.25–[11]	0.33–[10]
Heilongjiang	0.34–[7]	0.46–[5]
Shiyan	0.23–[15]	0.31–[14]
Neimenggu	0.36–[17]	0.47–[16]

Continued on next page

Table 2 – continued from previous page

Province/City	$R_t^{10.5}$	R_t^{14}
Xiaogan	0.28–[14]	0.37–[13]
Xinjiang	0.42–[12]	0.56–[10]
Beijing	0.13–[11]	0.18–[9]
Jingzhou	0.19–[8]	0.25–[3]
Shaanxi	0.14–[17]	0.18–[16]
Chongqing	0.13–[11]	0.17–[10]
Henan	0.2–[9]	0.26–[8]
Hebei	0.26–[5]	0.35–[3]
Guangxi	0.17–[12]	0.23–[7]
Shanghai	0.16–[18]	0.21–[16]
Jiangsu	0.2–[10]	0.26–[6]
Jilin	0.11–[7]	0.15–[7]
Fujian	0.11–[13]	0.15–[11]
Shanxi	0.09–[16]	0.13–[14]
Yichang	0.17–[17]	0.22–[14]
Yunnan	0.2–[21]	0.26–[19]
Anhui	0.16–[8]	0.21–[7]
Xianning	0.47–[8]	0.63–[8]
Suizhou	0.18–[16]	0.25–[16]
Shandong	0.14–[12]	0.19–[9]
Guangdong	0.17–[10]	0.23–[9]
Xiangyang	0.12–[17]	0.16–[15]
Zhejiang	0.04–[18]	0.06–[17]
Enshizhou	0.2–[12]	0.27–[4]
Huanggang	0.07–[10]	0.09–[7]
Guizhou	0.11–[4]	0.15–[3]
Jingmen	0.12–[8]	0.16–[4]
Gansu	0–[7]	0–[6]
Hainan	0.03–[8]	0.04–[7]
Hunan	0.02–[10]	0.07–[9]
Ningxia	0.18–[9]	0.24–[9]
Huangshi	0.13–[8]	0.17–[7]
Jiangxi	0.12–[9]	0.16–[7]
Liaoning	0.08–[20]	0.11–[16]

Continued on next page

Table 2 – continued from previous page

Province/City	$R_t^{10.5}$	R_t^{14}
Qinghai	0–[4]	0–[4]

499

Table 3: The 95% prediction intervals for the ending times, and the final accumulative number of infected cases of COVID-19 epidemic in the 30 provinces based on data to Feb 19 2020 with $\gamma = 0.1$. The last column lists the total infected cases ($I(t) + R(t)$) as Feb 19, 2020.

Province	Ending time	\hat{N}_{final}	Current
Hubei	6/20 - 6/21	73857 - 74596	62322
Guangdong	4/27 - 4/29	1368 - 1412	1347
Zhejiang	4/26 - 4/27	1225 - 1245	1195
Beijing	4/17 - 4/20	416 - 436	397
Chongqing	4/18 - 4/21	581 - 600	565
Hunan	4/21 - 4/23	1028 - 1046	1021
Guangxi	4/11 - 4/15	254 - 271	248
Shanghai	4/12 - 4/16	345 - 365	336
Jiangxi	4/23 - 4/25	969 - 994	955
Sichuan	4/25 - 4/28	589 - 619	525
Shandong	4/19 - 4/21	567 - 584	553
Anhui	4/26 - 4/28	1044 - 1068	1006
Fujian	4/13 - 4/16	306 - 320	299
Henan	4/29 - 5/1	1358 - 1387	1283
Jiangsu	4/20 - 4/23	662 - 687	640
Hainan	4/6 - 4/9	174 - 183	168
Tianjin	4/7 - 4/14	141 - 159	132
Yunnan	4/7 - 4/11	174 - 187	174
Shaanxi	4/12 - 4/16	262 - 276	250
Heilongjiang	4/23 - 4/26	519 - 554	479
Liaoning	3/31 - 4/3	120 - 126	122
Guizhou	4/4 - 4/10	150 - 165	147
Jilin	3/30 - 4/4	93 - 101	92
Ningxia	3/18 - 3/26	65 - 73	71
Hebei	4/12 - 4/16	319 - 336	312
Gansu	3/20 - 3/26	90 - 96	92
Xinjiang	3/31 - 4/9	78 - 96	78

Continued on next page

Table 3 – continued from previous page

Province	Ending time	\hat{N}_{final}	Current
Shanxi	4/1 - 4/5	134 - 142	134
Neimenggu	4/2 - 4/11	78 - 98	76
Qinghai	2/23 - 3/6	17 - 20	19

500

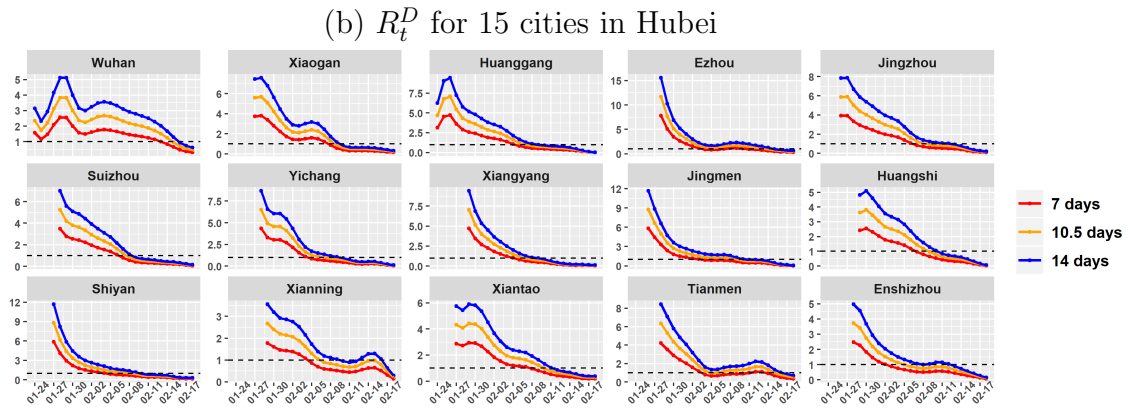
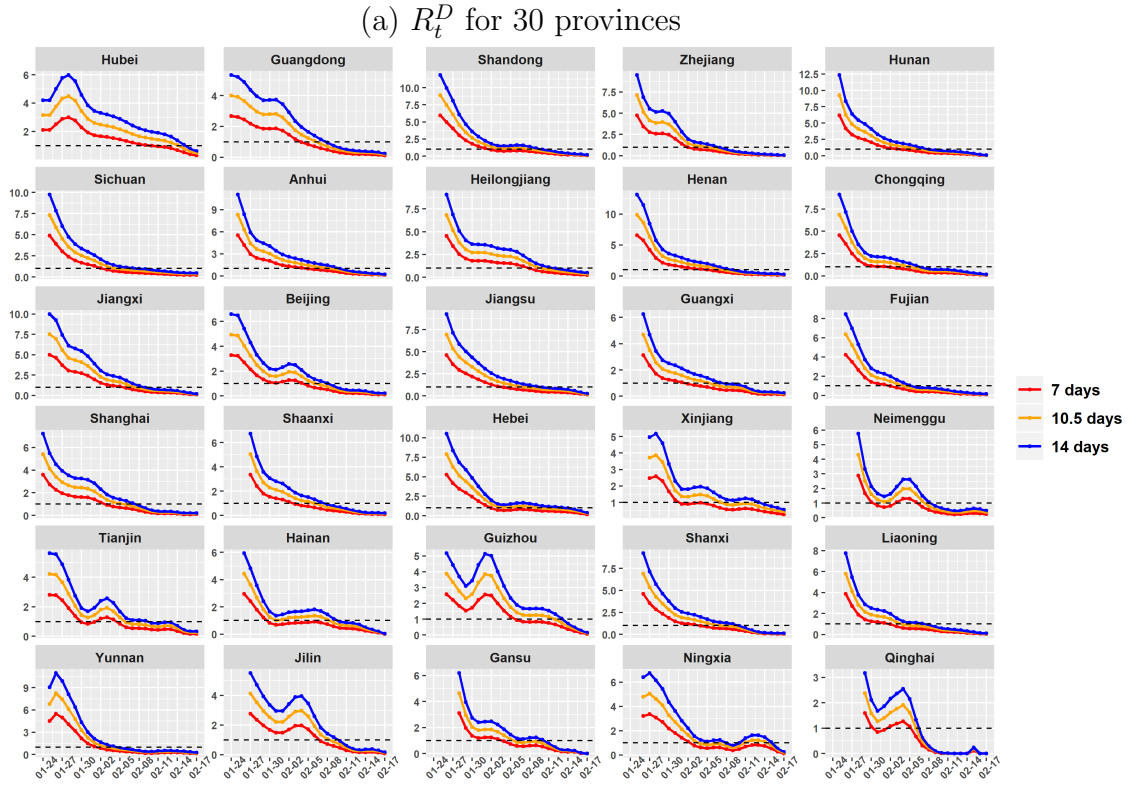
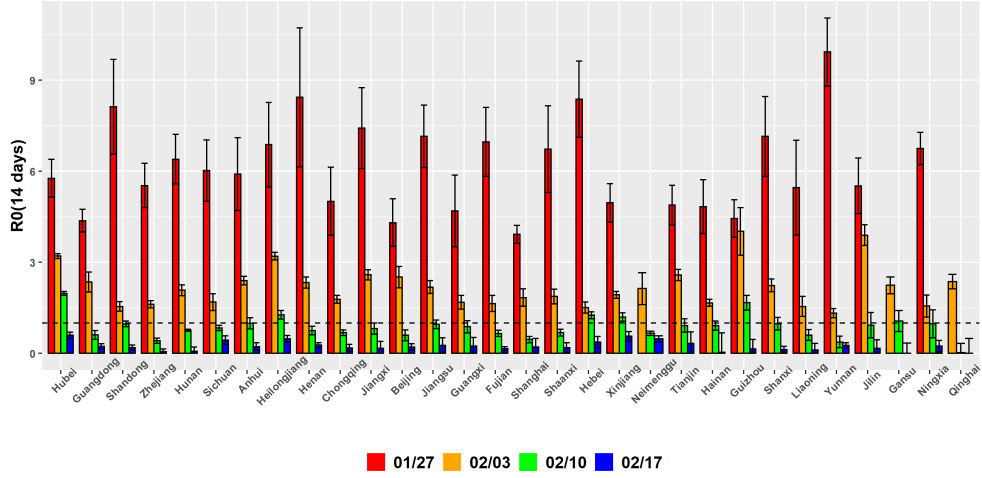


Figure 1: Time series of the reproduction number R_t^D at three infectious durations: $D = 7$ (red), 10.5 (orange), 14 (blue), for the 30 mainland provinces (a) and the 15 cities in Hubei province (b) from Jan 21 to Feb 17 2020. The black horizontal line is the critical threshold level 1.

(a) R_t^{14} for 30 provinces



(b) R_t^{14} for 15 cities in Hubei

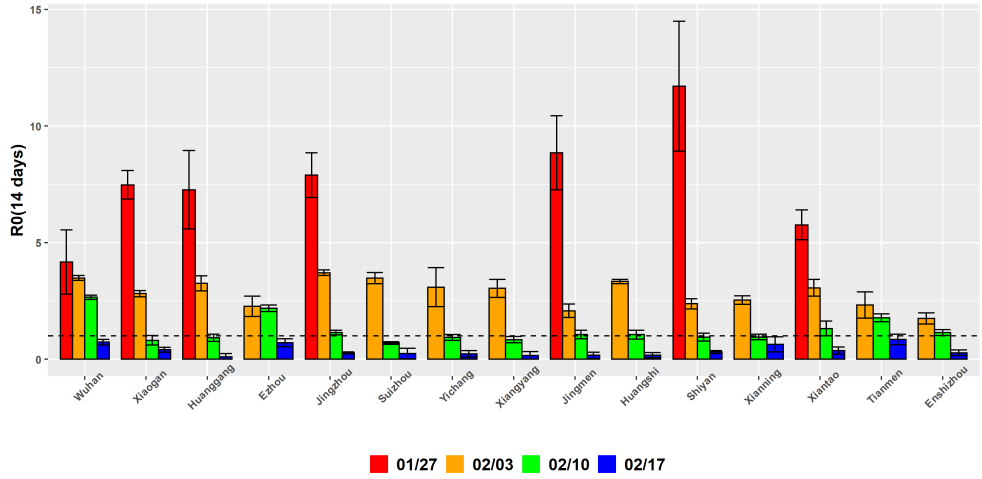


Figure 2: Elevated 95% confidence intervals (black) of the 14-day R_t for the 30 mainland provinces (a) and the 15 Hubei cities (b) on Jan 27 (red), Feb 3 (orange), Feb 10 2020 (green) and Feb 17 (blue). The black horizontal lines mark the critical threshold 1.

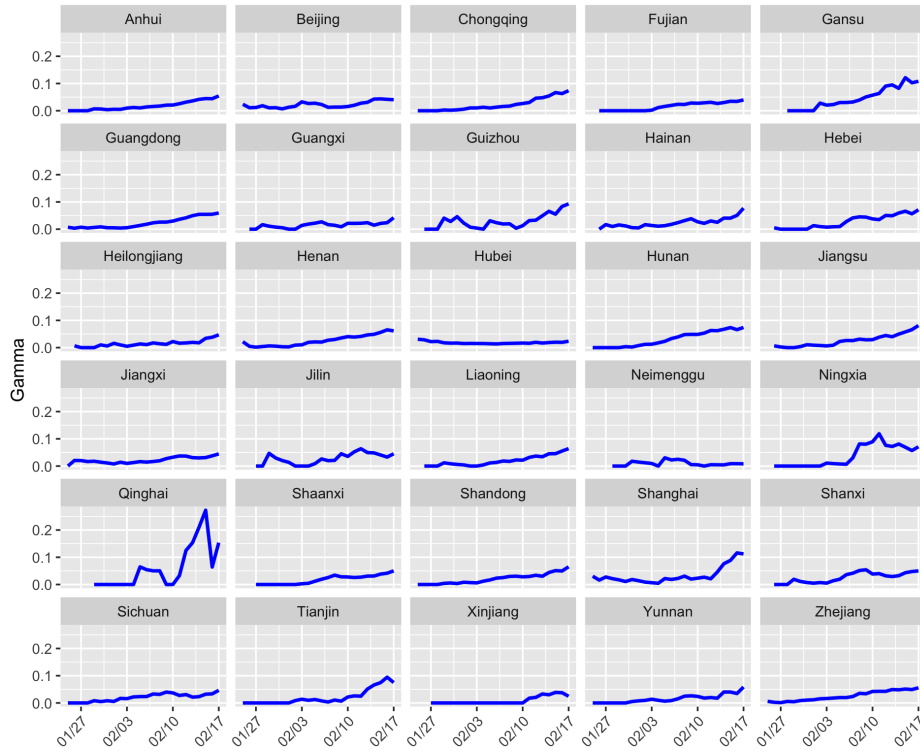


Figure 3: The estimated $\hat{\gamma}(t)$ from the varying coefficient SIR model (1) for the data to Feb 17th 2020 for 30 provinces.

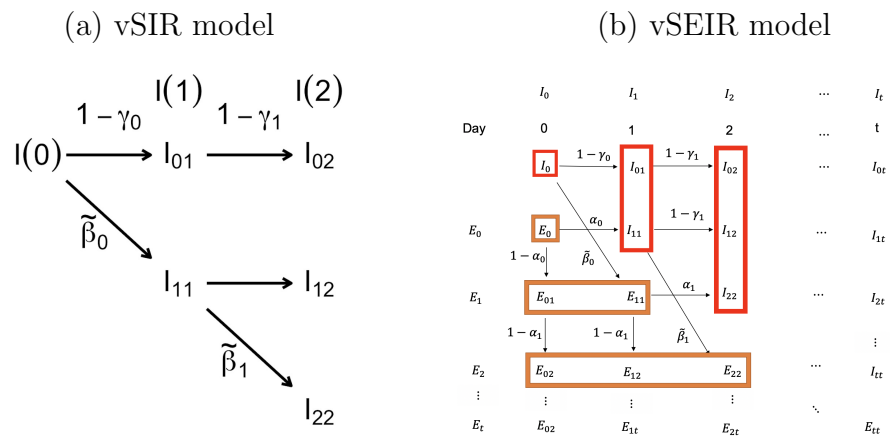


Figure 4: Epidemic progression networks under vSIR and vSEIR models

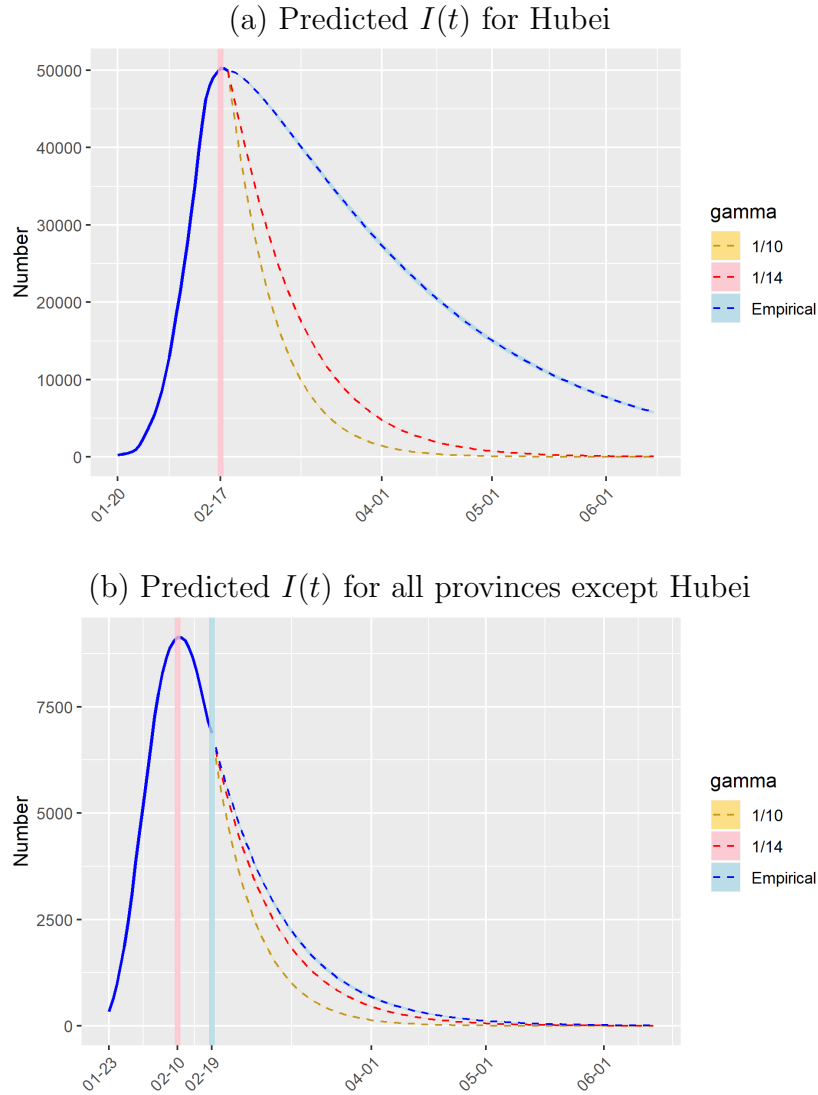


Figure 5: Predicted number of infected cases $I(t)$ with 95% prediction interval for Hubei Province in panel (a) and all other provinces combined except Hubei in panel (b). The grey vertical line indicates the current date of observation; the blue solid line plots the observed $I(t)$ before Feb 19th; the blue dashed line gives the predicted $I(t)$ with 95% prediction interval (blue shaded area) with the estimated $\hat{\gamma}_T$; the pink vertical line indicates the peak date of $I(t)$; the orange and red dashed line gives the predicted $I(t)$ with 95% prediction interval (shaded area) with fixed recovery rate $\gamma = 0.1$ and $\gamma = 1/14$ respectively.